  Bull. Chem. Soc. Jpn., 61, 745—751 (1988)

Interference Effects of Helium on Motion of Xenon in Micropores of 5A Zeolites

Yusuke YASUDA* and Satoshi SHINBO
Faculty of Science, Toyama University, Toyama 930
(Received June 22, 1987)

Striking interference effects of He molecules on the motion of Xe in micropores of 5A zeolites have been found by the frequency response method. Results of the systems reveal that the absorbed Xe molecules may be divided into two abspecies, c_1' and c_2', in the presence of He molecules which were inert in a single component system: (i) at 273 K, c_1' diffuses faster and c_2' slower than pure Xe; (ii) at 255 K, c_1' diffuses faster than pure Xe, while the motion of c_2' is regarded as not diffusion but adsorption. The interference effects at 273 K have been explained quantitatively by decoupling a more general form of Fick's law containing cross terms.

Since zeolites have a molecular-sieve action, the binary or multicomponent diffusion of gases in the micropores of zeolites has been of considerable interest after the discovery of zeolite crystals in the late 1950s. However, conclusions seem controversial: (i) the diffusion of one component is enhanced in a mixture,[1] (ii) both diffusion coefficients of a binary gas mixture are considerably smaller than those of pure components,[2] and (iii) each component of a mixture (using He as a carrier gas) diffuses independently with the same intrinsic mobility as for single-component diffusion.[3]

In the first application of the frequency response (FR) method to a system of a binary gas mixture, CH_4+He or CH_4+Kr over Linde 5A at 195 K, striking mutual interference effects have been observed in the diffusion process.[4] The aim of the present article is to confirm that the interference occurs in micropores rather than on the exposed surface of a zeolite. The dependence of the effects on the crystal size of a zeolite was investigated using simpler gas systems of Xe+He over two kinds of 5A zeolites, Ca-A2 and Ca-A6, of which the mean crystal sizes were 2 and 6 μm, respectively.

Experimental

Zeolite Preparation and Materials. Synthetic 5A zeolites supplied by Toyo Soda Manufacturing Co., Ca-A2 and Ca-A6, were used; their properties are summarized in Table 1. SEM photographs of the samples are shown in Fig. 1. Crystal-size distributions of the two samples were determined by measuring the size of ca. 700 crystals; that of Ca-A2 was practically normal on a weight or volume fraction basis, but that of Ca-A6 was distorted.

Table 1. Cation Exchange and Size Distribution of 5A Zeolite Crystals

Zeolite	%Ca[a]	N[b]	$(2a_m/\mu m)$[c]	(σ/a_m)[d]
Ca-A2	96	660	1.7	0.28
Ca-A6	94	800	5.5	0.4

a) Expressed as % of original Na^+ ions replaced by Ca^{++}. b) Number of particles measured. c) Mean cube side. d) Relative standard deviation.

Powders were first pelleted under a pressure of ca. 1×10^3 kg cm^{-2}, crushed, and dehydrated at 383 K for 10 h. The temperature was then raised to 623 K and the system evacuated at that level for at least 20 h. Practically the same FR results were obtained for samples both with and without compression.

No impurities were detected in the Xe or He by mass spectrometer analysis.

Apparatus and Procedure. The FR apparatus was described in a previous paper.[4] The gas space V of the system was varied sinusoidally as

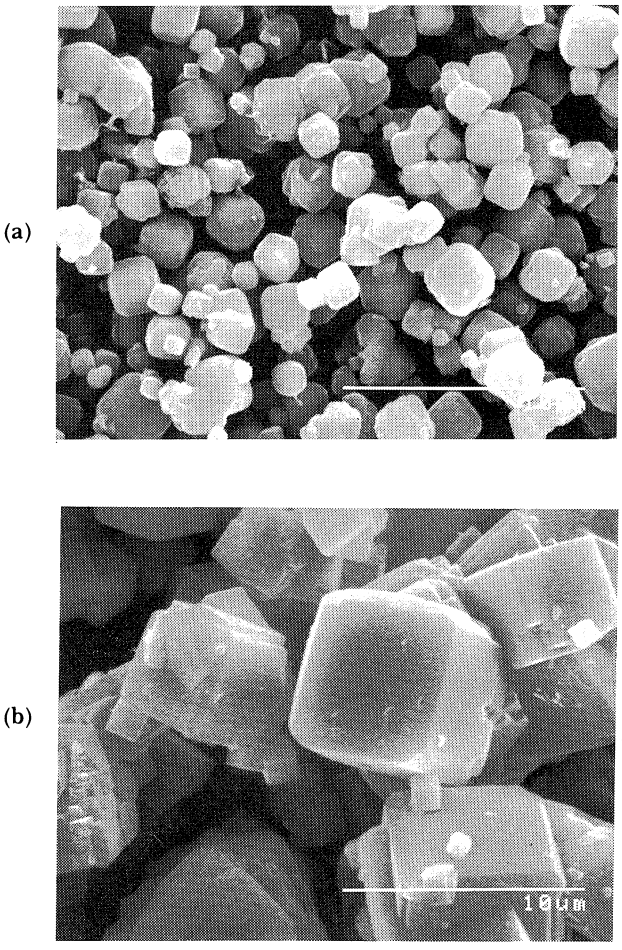

Fig. 1. SEM photographs of (a) Ca-A2 and (b) Ca-A6 zeolites.

$$V(t) = V_e(1 - ve^{i\omega t}), \quad (1)$$

where V_e is the equilibrium or the mean volume of the oscillation, v the relative amplitude and ω the angular velocity. The induced pressure variation can be well expressed by

$$P(t) = P_e\{1 + pe^{i(\omega t+\varphi)}\}. \quad (2)$$

In order to remove any apparent change in the p or φ characteristic of the apparatus due to a delay of the pressure-gauge reading, blank experiments were carried out without zeolites.

Actual values of v and φ were determined by

$$v = p_B \text{ and } \varphi = \varphi' - \varphi_B, \quad (3)$$

where p_B and φ_B denote the results obtained in a blank experiment carried out under almost the same conditions for P_e, T_e, and further at the same ω. φ' is the value of raw data obtained in a system with zeolites.

The various conditions for the pure Xe and Xe+He systems should be regarded as identical, since after each run of ω's for a pure Xe system was completed, small amounts of He were introduced into the system while repeating the scanning of ω. The (total) equilibrium pressure, P_e, was measured using a conventional mercury manometer.

Results

Dependence of p/v and φ on ω. In preliminary experiments for pure He systems, various results agreed with those of the blank experiments. It is concluded, therefore, that

$$p/v = 1 \text{ and } \varphi = 0 \quad (4)$$

with respect to the pure He system.

The results of p/v and φ obtained from single and binary gas systems of Ca-A2 at 273 K are shown in Figs. 2(a) and 2(b), for which the experimental conditions are given in Table 2.

If both Xe and He molecules behave independently in the mixture, the values of p/v and φ corresponding to ΔP_T in Fig. 3 are expected to be intermediate of those corresponding to ΔP_{Xe} and ΔP_{He} (as illustrated in Fig. 3). Calculated results from the triangle are represented by the dashed curves in Figs. 2(a) and 2(b). The discrepancy between the two dashed curves, one

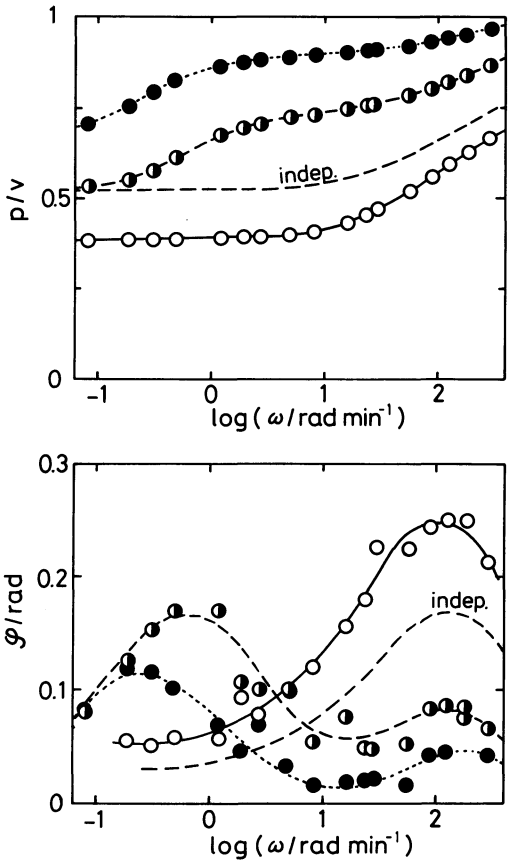

Fig. 2. Raw data of Xe and Xe+He mixtures over Ca-A2 at 273 K; (a) p/v and (b) φ versus ω. ○, pure Xe(Exp. No. 1); ◑, Xe:He=4:1(Exp. No. 2); ●, Xe:He=4:3(Exp. No. 3). The dashed curves indicated by "indep." represent calculated results under the assumption that each component of Xe:He=4:1 behaves independently.

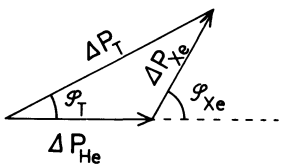

Fig. 3. Relations among total and partial pressure variation; $P_T(t)=P_T^{(e)}+\Delta P_T\cos(\omega t+\varphi_T)$, $P_{He}(t)=P_{He}^{(e)}+\Delta P_{He}\cos(\omega t+0)$, and $P_{Xe}(t)=P_{Xe}^{(e)}+\Delta P_{Xe}\cos(\omega t+\varphi_{Xe})$. An equality of $P_T(t)=P_{He}(t)+P_{Xe}(t)$ leads to the triangle.

Table 2. Summary of Experimental Conditions

Exp. No.	T_e/K	Absorbent	P_{Xe}[a]/Torr	P_{He}[a]/Torr	Xe molecule per cavity	K_T[b]
1	273	Ca-A2[d]	3.6	0	0.9×10^{-1}	(1.93)[c]
2			3.6	1.0		1.05
3			3.6	3.1		0.55
4		Ca-A6[e]	3.1	0	1.2×10^{-1}	(2.90)
5			3.1	1.1		1.23
6	255	Ca-A2	4.1	0	2.2×10^{-1}	(4.75)
7			4.1	1.2		1.77
8		Ca-A6	3.6	0	3.3×10^{-1}	(8.05)
9			3.6	0.9		2.39

a) Partial pressure of each component (1 Torr=133.322 Pa). b) Calculated from the gradient of absorption isotherm according to Eq. 9. c) $=K_2^{(0)}$. d) 7.84 g in a dehydrated state. e) 7.85 g in a dehydrated state.

experimental and the other calculated, suggests considerable interference effects between Xe and He. It should be noted that the *single* peak in φ's of the pure Xe system seems to split into *two* peaks in the presence of "inert" (see Eq. 4) molecules of He.

Frequency Response of the Systems. Results at 273 K: The in-phase and out-of-phase components of the FR, $(v/p)\cos\varphi$-1 and $(v/p)\sin\varphi$, respectively, which were calculated from the data in Figs. 2(a) and 2(b), are shown in Figs. 4(a) and 4(b). In order to demonstrate the effects of He, they are divided by a constant K_T (Table 2).

The value of K_T for a single-component system was determined by the gradient of the absorption isotherm:[5]

$$K_T = \frac{RT_0}{V_e}\left(\frac{dB^{(0)}}{dP}\right)_e, \qquad (5)$$

where B denotes the amount of abspecies and the superscript, (0), indicates the value in a pure gas system.

The value of K_T of a multicomponent system may be given by (Appendix 1)

$$K_T = \frac{\sum_m x_m K_m/(K_m+1)}{\sum_n x_n/(K_n+1)}, \qquad (6)$$

where x_m denotes the mole fraction of the m-component in the *gas* phase. K_m is defined as

$$K_m = \frac{RT_0}{V_e}\left(\frac{dB_m}{dP_m}\right)_e, \qquad (7)$$

where B_m denotes the amount of the m-molecules absorbed; P_m is the partial pressure of the component.

In the present work, the absorption isotherm of pure Xe was practically unaltered by the addition of He. Therefore, the values of K_1 and K_2 (the subscript 1 and 2 refer to He and Xe, respectively) can be determined by those obtained in the single-component system:

$$K_1 = K_1^{(0)} (= 0)$$

and

$$K_2 = K_2^{(0)}\left(= \frac{RT_0}{V_e}\left(\frac{dB_2^{(0)}}{dP}\right)_e\right). \qquad (8)$$

The amount of Xe molecules, $B_2^{(0)}$, was proportional to the equilibrium pressure. The constants of $K_2^{(0)}$ are given in Table 2. Consequently, K_T of the binary gas mixture can be evaluated by

$$K_T = \frac{x_2 K_2^{(0)}}{1 + x_1 K_2^{(0)}}. \qquad (9)$$

The values of K_T, thus obtained, are given in Table 2; K_T is expected to be the upper limit of the in-phase components.[5]

Results of Ca-A6 are plotted in Figs. 5(a) and 5(b) together with those of Ca-A2 which were obtained

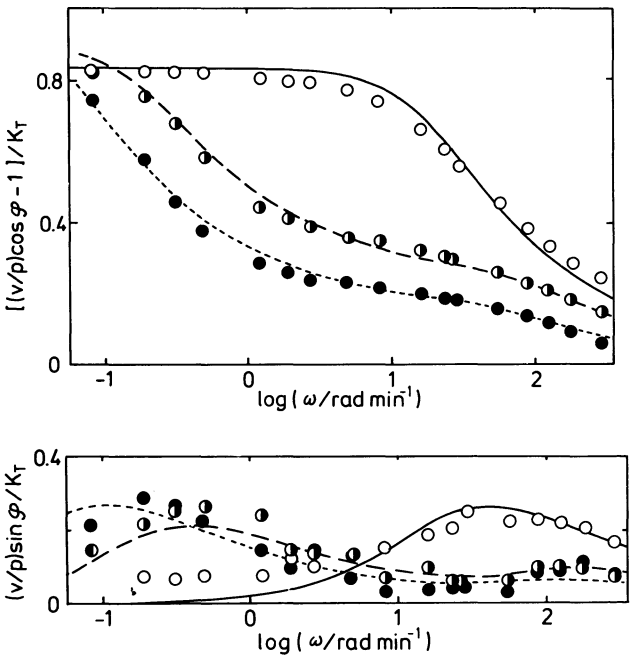

Fig. 4. Frequency response of Xe and Xe+He mixtures over Ca-A2 at 273 K; (a) in-phase and (b) out-of-phase components normalized by K_T versus ω. Notation is that of Fig. 2. Various curves represent calculated results according to Eqs. 10 and 11 with the parameters given in Table 3.

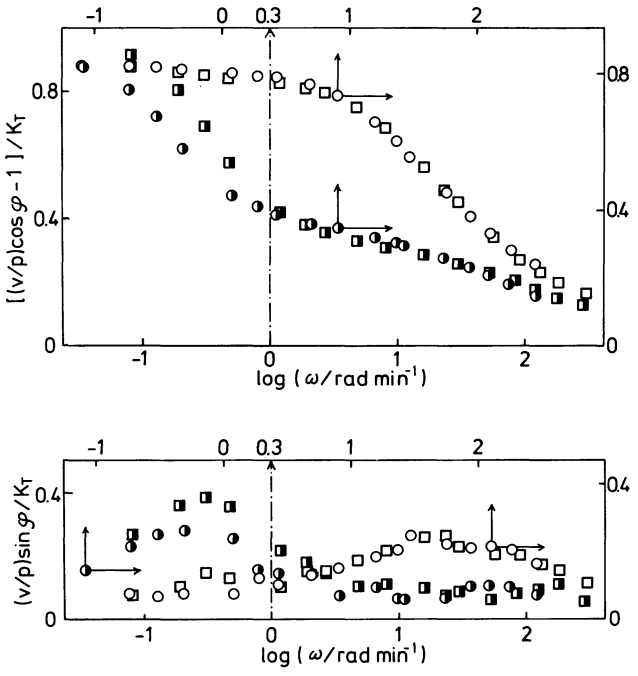

Fig. 5. Dependence of crystal size on FR of the systems; (a) in-phase and (b) out-of-phase components normalized by K_T versus ω. Squares are the results obtained from Ca-A6 systems; □, pure Xe (Exp. No. 4); ◨, Xe:He=3:1(Exp. No. 5). Circles correspond to those in Fig. 4.

under similar conditions; they were almost superimposable by being moved parallel to the abscissa of 0.30.

Results at 255 K: Similar experiments were carried out at 255 K. Their experimental conditions are summarized in Table 2. The values of FR of the various systems are shown together in Fig. 6. It is worthwhile noting that the results obtained in the lower ω region seem to be independent of the crystal size, whereas those in the higher ω region depend on it.

FR Data Analysis

FR at 273 K. On the basis of the experimental results, it is assumed that *two* diffusion processes are involved in the binary gas systems, so that the FR may be described by[4]

$$\{(v/p)\cos\varphi - 1\}/K_T = \tilde{K}_1\bar{\delta}_{3c}(2\omega a_m^2/D_1') + \tilde{K}_2\bar{\delta}_{3c}(2\omega a_m^2/D_2') \quad (10)$$

and

$$(v/p)\sin\varphi/K_T = \tilde{K}_1\bar{\delta}_{3s}(2\omega a_m^2/D_1') + \tilde{K}_2\bar{\delta}_{3s}(2\omega a_m^2/D_2'), \quad (11)$$

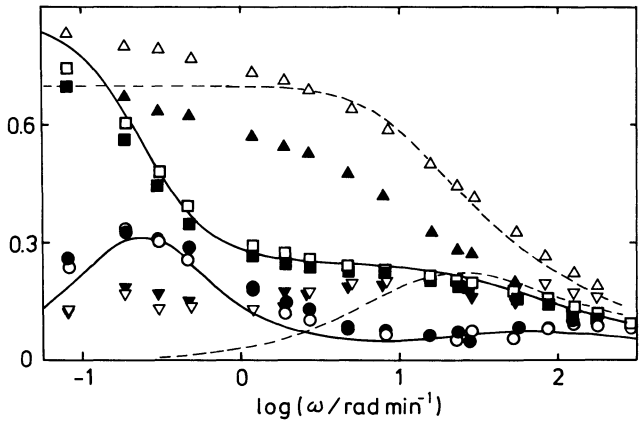

Fig. 6 Frequency response of Xe and Xe+He mixtures over Ca-A2 (open symbols) and Ca-A6(solid symbols) at 255 K. △(Exp. No. 6) and ▲(Exp. No. 8), in-phase(normalized) components of pure Xe systems; ▽ and ▼, out-of-phase(normalized) components of the same systems. □(Exp. No. 7) and ■(Exp. No. 9), the in-phase components of Xe:He=4:1 systems; ○ and ●, the out-of-phase components of the same systems. The solid curves represent calculated results according to Eqs. 13 14 with the parameters of $\tilde{K}_1$=0.25, D_1'/a_m^2=6.2 min^{-1}, $\tilde{K}_2$=0.63, and κ_{-2}=0.24 min^{-1}.

where $\tilde{K}_i$ is a constant giving the fraction of the i-th term; D_i' is the Fickian diffusivity.

The characteristic functions of $2\omega a_m^2/D_i'$ for the diffusion process, $\bar{\delta}_{3c}$ and $\bar{\delta}_{3s}$, were computed using

$$\bar{\delta}_{3j}(2\omega a_m^2/D_i') = \frac{1}{\sqrt{2\pi}\,\sigma}\int_0^\infty [\delta_{3j}(2\omega a^2/D_i') \exp\{-\frac{(a-a_m)^2}{2\sigma^2}\}]\,da, \quad (12)$$

(j = c or s)

where the values of a_m and σ in Table 1 were inserted. Two analytical functions of x, $\delta_{3c}(x)$, and $\delta_{3s}(x)$, were given explicitly in a previous paper.[5]

The theoretical results, thus calculated, are represented by various curves in Figs. 4(a) and 4(b), of which the parameters determined on a trial and error basis ($\tilde{K}_1$, D_1'/a_m^2, $\tilde{K}_2$, and D_2'/a_m^2) are summarized in Table 3.

FR at 255 K. Results obtained at 255 K could not be reproduced by the two-diffusion model of Eqs. 10 and 11. However, they seem to be described by

$$\{(v/p)\cos\varphi - 1\}/K_T = \tilde{K}_1\bar{\delta}_{3c}(2\omega a_m^2/D_1') + \tilde{K}_2\frac{1}{1+(\omega/\kappa_{-2})^2} \quad (13)$$

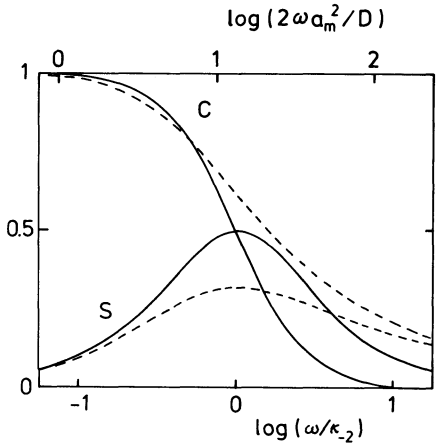

Fig. 7. Comparison of two kinds of characteristic functions: solid curves represent $1/\{1+(\omega/\kappa_{-2})^2\}$ (C) and $(\omega/\kappa_{-2})/\{1+(\omega/\kappa_{-2})^2\}$ (S) applicable to an adsorption-desorption process; dashed curves are $\bar{\delta}_{3c}$ (C) and $\bar{\delta}_{3c}$ (S) applicable to the diffusion process in Ca-A2(σ=0.28).

Table 3. Parameters for $\tilde{K}_i$ and D_i'/a_m^2 in Eqs. 10 and 11

Exp. No.	$\tilde{K}_1$	(D_1'/a_m^2)/min^{-1}	$\tilde{K}_2$	(D_2'/a_m^2)/min^{-1}
1	(0.83	3.05)		
2	0.23	18.1	0.67	3.0×10^{-2}
3	0.15	11.9	0.85	8.0×10^{-3}

and

$$(v/p)\sin\varphi/K_T = \tilde{K}_1\bar{\delta}_{3s}(2\omega a_m^2/D_1') + \tilde{K}_2\frac{(\omega/\kappa_{-2})}{1+(\omega/\kappa_{-2})^2}. \quad (14)$$

Each second term on the right hand side is a characteristic function for the adsorption-desorption process,[6] which is compared with $\bar{\delta}_{3c}$ or $\bar{\delta}_{3s}$ in Fig. 7; evidently they are very different.

The theoretical results for the systems of Ca-A2 are represented by the solid curves in Fig. 6.

Discussion

Pure Xe Systems. Almost all abspecies of Xe (more than 80%, see Fig. 4(a)) may be regarded as identical; the out-of-phase components could be reproduced by the solid curve stemming from a single term in Eq. 10 (see Table 3). The moved distance (0.30) in Figs. 5(a) and 5(b), on the other hand, leads to

$$\frac{D_2^{(0)}/a_m^2 \text{ of Ca-A2}}{D_2^{(0)}/a_m^2 \text{ of Ca-A6}} = 2.0, \quad (15)$$

where $D_2^{(0)}$ denotes the Fickian diffusivity of a pure Xe system. Substitution of the values of a_m's leads to

$$\begin{aligned} D_2^{(0)}/10^{-14}\,\mathrm{m^2\,s^{-1}} &= 3.7 \quad \text{for Ca-A2} \\ &= 19 \quad \text{for Ca-A6} \\ (&= 15 \quad \text{for Linde-5A})^{7} \end{aligned} \quad (16)$$

Contrary to our expectation, the difference in this diffusivity was considerable. It is noted, however, that the absorption isotherm of these two kinds of zeolites were considerably different (see $K_2^{(0)}$'s in Table 2). The diffusivities for small commercial zeolite crystals were found to be substantially smaller than for large laboratory synthesized crystals.[8] The reproducibility of the theoretical curves at 255 K was not so good (see dashed curves in Fig. 6).

Binary Gas Systems. Since the FR of mixture was affected by the change in the crystal size, the interference effects due to He would be attributed to processes occurring not on exposed surfaces, but within micropores.

The experimental results can be summarized as follows: (i) there is only one diffusion process in the pure Xe system, (ii) no FR of He was observed in a pure He system since the absorption of He was negligible and, thus, $K_1^{(0)}=0$ and (iii) (only) two diffusion processes were needed to theoretically reproduce FR data on a binary gas system. On the basis of these results, a more general form of Fick's law,

$$\frac{\partial c_m}{\partial t} = \sum_{n=1}^{2} D_{mn}\nabla^2 c_n, \qquad m = 1 \text{ or } 2 \quad (17)$$

is assumed. Here, c_m denotes the concentration of the m-component and D_{mn} is the Fickian diffusivity ($D_{11}>D_{22}$). Every D_{mn} would depend on both c_1 and c_2. However, since the perturbation of the FR method was very small (e.g. $v\sim10^{-2}$) and, therefore, $c_m\fallingdotseq c_m^{(e)}$, D_{mn} can be regarded as a constant.

The coupled equations may be decoupled by the transformations:

$$c_1' = \{1+(D_-/D_+)\}c_1 + (D_-/D_+)c_2 \quad (18)$$

and

$$c_2' = -(D_-/D_+)c_1 + \{1-(D_-/D_+)\}c_2. \quad (19)$$

In these equations the short notations

$$D_+ \equiv D_{21} + D_{12} \quad (20)$$

and

$$D_- \equiv D_{21} - D_{12} \quad (21)$$

are introduced.

Substitution of c_m' for c_m in Eq. 17 leads to

$$\frac{\partial c_m'}{\partial t} = D_m'\nabla^2 c_m' \qquad m = 1 \text{ or } 2, \quad (22)$$

where

$$D_1' = D_{11} + \frac{1}{2}D_-, \quad (23)$$

and

$$D_2' = D_{22} + \frac{1}{2}D_-. \quad (24)$$

The values of D_i' in Table 3 are expected to correspond to these eigenvalues.

In the present work, c_1 is sufficiently small. A comparison of Eqs. 18 and 19 with Eqs. 10 and 11 would lead to

$$\frac{\tilde{K}_1}{\tilde{K}_2} = \frac{(D_-/D_+)}{1-(D_-/D_+)}. \quad (25)$$

When the value of D_-/D_+ is found from the $\tilde{K}_i$'s (Table 3) all four coefficients, D_{mn}, can be evaluated successively (Appendix 2). The derived values are given in Table 4 and are plotted in Fig. 8.

Since the values of (D_{mn}/a_m^2)'s were determined after many steps of calculation from the raw data on $K_2^{(0)}$, P_e, ΔP, and φ, their absolute values are not very reliable; the ambiguity estimated is indicated by the vertical lines in Fig. 8 (most of the ambiguity would arise from errors in P_e's in the present work). However, the conclusions that

$$D_{12} \fallingdotseq D_{21} \fallingdotseq (D_{11}D_{22})^{1/2} \quad (26)$$

Table 4. Values of D_{mn}/a_m^2 Derived (in $\mathrm{min^{-1}}$ Units)

Exp. No.	D_{11}/a_m^2	D_{12}/a_m^2	D_{21}/a_m^2	D_{22}/a_m^2
2	16.9	3.44	5.80	1.21
3	11.6	1.51	2.05	0.28

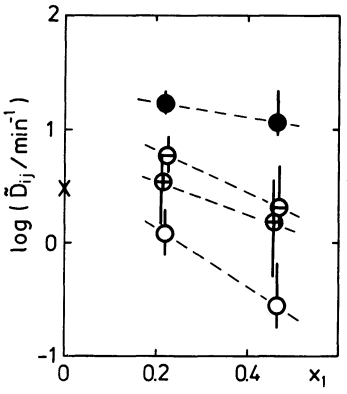

Fig. 8. Diffusional time constant $\tilde{D}_{ij}$'s of Xe+He/Ca-A2 systems at 273 K versus the mole fraction of He in gas phase, x_1. ●, $\tilde{D}_{11}$; ⊕, $\tilde{D}_{12}$; ⊖, $\tilde{D}_{21}$; ○, $\tilde{D}_{22}$, where $\tilde{D}_{ij}=D_{ij}/a_m^2$. × indicates the value of pure Xe.

and

$$D_{12} < D_{21} \tag{27}$$

should be reliable, since they are governed by the values of D_1'/a_m^2 and the *ratio* of $\tilde{K}_1/\tilde{K}_2$.

Four constants of D_{mn}'s with respect to a heptane+benzene over NaX system have been determined empirically by a sorption method.[9] The results lead to

$$D_{12} > D_{21} \tag{28}$$

in contrast to the result of Eq. 27, though the method is based on the supposition that all D_{mn}'s do not depend on the concentrations.

The cross-terms, D_{12} and D_{21}, have been determined by a random-walk approach.[10] The application of the method to a simultaneous sorption of two sorbates in an initially empty pore system shows very significant multicomponent effects due to the contribution of the cross terms.

In summary, Xe molecules in micropores may be divided into two species in a Xe+He mixture; the division into c_1' and c_2' species depends on the ratio of D_-/D_+; one of the two species becomes an adspecies with decreasing temperature.

Appendix 1

Since the vapor may be regarded as ideal,

$$p_T = x_1 p_1 + x_2 p_2, \tag{A1}$$

where the subscript T indicates the value of the total pressure. On the other hand, in consideration of a case at $\omega \fallingdotseq 0$, one finds

$$v - p_{0T} = K_1 x_1 p_{01} + K_2 x_2 p_{02}, \tag{A2}$$

where the subscript 0 indicates the value in the quasistatic state.

The asymptotic value of the in-phase component, K_T, is given by

$$K_T = (v/p_{0T}) - 1 \tag{A3}$$

since φ tends to zero as $\omega \to 0$. In the same way,

$$K_i = (v/p_{0i}) - 1. \tag{A4}$$

Eliminating p_{0T}, p_{01}, and p_{02}, one finds

$$K_T = \frac{\sum_{m=1}^{2} x_m K_m/(K_m+1)}{\sum_{n=1}^{2} x_n/(K_n+1)} = \frac{K_1K_2 + x_1K_1 + x_2K_2}{1 + x_1K_2 + x_2K_1}. \tag{A5}$$

Appendix 2

Other parameters, D' and d, are introduced:

$$D_{21} = D' + d \tag{A6}$$

and

$$D_{12} = D' - d \tag{A7}$$

or

$$D_+ = 2D' \tag{A8}$$

and

$$D_- = 2d. \tag{A9}$$

The ratio D_-/D_+ or d/D' is replaced by δ for simplicity:

$$D_-/D_+ = d/D' = \delta. \tag{A10}$$

Equations 23 and 24 lead to

$$D_1' - D_2' = D_{11} - D_{22} + D_-. \tag{A11}$$

In the transformation of Eqs. 18 and 19, the relation

$$c_1' + c_2' = c_1 + c_2 \tag{A12}$$

is always satisfied. This necessary condition requires a relation among the D_{mn}'s:

$$D_+^2 = 2D_-(D_{11} - D_{22} + D_-). \tag{A13}$$

Substitution of Eq. A10 into Eq. A13 leads to

$$D' = \delta(D_1' - D_2'). \tag{A14}$$

When δ is determined, Eq. A14 gives D' and Eq. A10 gives the value of d. Consequently, the four coefficients may be determined as

$$D_{11} = D_1' - d, \tag{A15}$$

$$D_{12} = D' - d, \tag{A16}$$

$$D_{21} = D' + d, \tag{A17}$$

and

$$D_{22} = D_2' + d. \tag{A18}$$

Notation

a : radius of an isotropic sphere (cubic crystals are approximated by the sphere).

a_m : mean radius of the sphere.

$B^{(0)}$: amount of molecules absorbed in a single component system.
B_m : amount of abspecies of m-component in a mixture.
c_m : concentration of abspecies of m-component in micropores.
$c_m^{(e)}$: c_m at an equilibrium.
c_i' : concentration of a mixed abspecies of c_1 and c_2 derived mathematically by decoupling coupled equations.
$D_2^{(0)}$: Fickian diffusivity of a pure Xe system.
D_i' : Fickian diffusivity of c_i'.
D_{mn} : Fickian diffusivity in a more general form.
$K_m^{(0)}$: coefficient calculated from the gradient of absorption isotherm of a pure gas system.
K_m : coefficient correlated to the gradient of absorption isotherm of m-component in a multicomponent system.
K_T : asymptotic value of the in-phase component at $\omega \rightarrow 0$ of a single or multicomponent system.
$\widetilde{K}_i$: coefficient indicating contribution of i-th characteristic function to FR data.
P : gas pressure.
P_e : P at an equilibrium.
P_m : partial pressure of m-component in a mixture.
p : relative amplitude of pressure variation.
T_e : equilibrium temperature of absorbent.
T_0 : (RT_0/V_e) is a conversion factor; T_0 is usually room temperature.
V : volume of gas space of a system.
V_e : V at an equilibrium.
v : relative amplitude of volume variation.
x_m : mole fraction of m-component in gas phase.

Greek Letters
δ_{3j} : characteristic function of diffusion for FR.
$\bar{\delta}_{3j}$: δ_{3j} modified by the crystal size distribution.
φ : phase lag between volume and pressure variation.
κ_{-2} : parameter characteristic of an adsorption-desorption process.
σ : standard deviation of a normal distribution.
ω : angular velocity of sinusoidal oscillation.

The SEM photographs were supplied by Toyo Soda Manufacturing Co.

References

1) H. W. Habgood, *Can. J. Chem.*, **36**, 1384 (1958).
2) Y. H. Ma and T. Y. Lee, *Ind. Eng. Chem., Fundam.*, **16**, 44 (1977).
3) R. Kumer, R. C. Duncan and D. M. Ruthven, *Can. J. Chem. Eng.*, **60**, 493 (1982).
4) Y. Yasuda, Y. Yamada, and I. Matsuura, Proc. 7th Int. Zeolite Conf., Tokyo, 1986. ed by Y. Murakami, A. Iijima, and J. W. Ward (Kodansha-Elsevier, Tokyo, 1986), p. 587.
5) Y. Yasuda, *J. Phys. Chem.*, **86**, 1913 (1982).
6) Y. Yasuda, *J. Phys. Chem.*, **80**, 1867 (1976).
7) Y. Yasuda and G. Sugasawa, *J. Catal.*, **88**, 530 (1984).
8) D. M. Ruthven, Principles of Adsorption and Adsorption Processes (John Wiley, New York, 1984) p. 150.
9) R. M. Marutovsky and M. Bülow, *Z. phys. Chem., Leipzing*, **263**, 849 (1982).
10) M. G. Palekar and R. A. Rajadhyaksha, *Chem. Eng. Sci.* **41**, 463 (1986).